



Modeling and Analyzing the Free Vibration of Simply Supported Functionally Graded Beam

Raghad Azeez Neamah^{1,2*} , Ameen Ahmed Nassar¹ , Luay Sadiq Alansari² 

1. University of Basrah  – College of Engineering – Mechanical Engineering Department – Basrah – Iraq. **2.** University of Kufa  – Faculty of Engineering – Mechanical Engineering Department – Najaf – Iraq.

*Correspondence author: ragada.deibel@uokufa.edu.iq

ABSTRACT

Euler, Timoshenko and high shear deformation theories to analyze the free vibration of the functionally graded (FG) beam were developed. The mechanical properties of this beam were assumed to differ in thickness direction according to the model of a power-law distribution. The principle of Hamilton was used to find equations of motion. For free vibration, the analytical solution of these equations was presented using the Navier method. The effect of power index, aspect ratio, modulus ratio, and deformation theories on dimensionless frequency were studied numerically by Ansys software and analytically according to different beam theories using the Fortran program. The obtained results from these programs were compared with each other and with some previous research. Results showed an excellent agreement with the previous research. The numerical and analytical results showed that the use of this new FG beam model especially based on first and high shear deformation theories leads to the reduction of dimensionless frequency. It may be concluded that, the including of shear's effect leads to a decrease in the dimensionless frequency. From the modeling and analysis of this model, it is possible to know what is the appropriate design for this FG beam model to reduce the vibration.

Keywords: Dimensionless frequency; Classical beam theory; First and high order shear deformation theories; power law model; Analytical and numerical methods.

INTRODUCTION

The properties of materials enhance with developments that occur day by day. Traditional materials available, such as metals, alloys, and composite materials, are suitable for specific applications (Fathi *et al.* 2020; Saleh *et al.* 2019). In the past, to develop these materials, homogeneous materials were manufactured, which were characterized by the optimum performance for most industrial applications (Saleh *et al.* 2020). However, to combine all the requirements of industrial development, it has become necessary to invent materials that are gradual in properties and structures for several fields, including engineering (aerospace and automobiles), medicine, and defense. These materials are characterized by gradation in their properties and structures in a specific direction (El-Galy *et al.* 2018; Li and Han 2018; Xu *et al.* 2019). Those materials are considered composite but heterogeneous substances called functionally graded (FG) materials (FGMs), which have several important properties like high toughness,

Received: Jan. 10, 2022 | Accepted: Apr. 19, 2022

Peer Review History: Single Blind Peer Review

Section editor: Renato Rebouças de Medeiros



This is an open access article distributed under the terms of the Creative Commons license.

thermal resistance, and low density (Chauhan and Khan 2014; Loy *et al.* 1999). In these materials, the volume fraction of each component is always various along the direction of thickness. Each component has different mechanical and thermal properties that lead to making them very suitable for various applications (Tarlochan 2012).

In 1984 these materials were designed and manufactured for the first time in the Japanese space shuttle to reduce the thermal stress of metal and ceramic interfaces due to the high temperature (Zainy *et al.* 2018). The idea of these materials is not new, as they are used in abundance in the human body, for example, in teeth, bones, and skin. These parts are characterized by gradual properties such as softness and hardness, in addition to the various functions that they perform (Sola *et al.* 2016).

Aydogdu and Taskin (2007) investigated the free vibration of simply supported (s-s) FG beam (FGB) depending on Timoshenko and different high order shear deformation theory (HSDT) together with the research developed by Rahmani *et al.* (2020) and Anandrao *et al.* (2012). Kapuria *et al.* (2008) studied experimentally the free vibration and static response of layered FGB of Ni/Al₂O₃ and Al/Sic arranged with powder metallurgy and combustion powder thermal spray respectively. Ke *et al.* (2010a) studied the nonlinear vibration of the FGB based on classical beam theory (CBT). Pradhan and Chakrartery (2013) presented the free vibration analysis of FGBs subjected to different boundary conditions. Rahimi *et al.* (2013) used the exact solution method to investigate the postbuckling of FGB. For nanobeams, the free vibration problem has been studied by using nonlocal beam theory and various shear deformation beam theories by Aydogdu (2009) and Elmeiche *et al.* (2016) respectively. Ke *et al.* (2010b) and El Bikri *et al.* (2012) studied the nonlinear free vibration of the FGB based on the Von Kármán geometrical nonlinearity assumptions. The material properties were assumed to change through-thickness agreeing to the rule of mixture. According to Euler Bernoulli's beam theory, the free vibration analysis of FG nanobeams modeled was presented by Eltaher *et al.* (2012).

The effect of nonlocal and material distribution parameters for different boundary conditions of nanobeams has been studied numerically. High order shear deformation theory for free vibration study of FGB and isotropic and FG sandwich beams was developed by Thai and Vo (2012) and Nguyen *et al.* (2015) respectively. Wattanasakulpong and Ungbhakorn (2012) applied different alteration methods to examine the free vibration of the FGB supported by random boundary conditions. Wattanasakulpong *et al.* (2012) used the third-order shear deformation theory to introduce a governing equation for predicting free vibration of layered FGB. Three types of layered numbers (5, 6, and 7) have been taken. Refined shear deformation theory to analyze the free vibration of the FGB was presented by Vo *et al.* (2013). Mohammadimehr and Mahmudian-Najafabadi (2013) studied the free vibration of the FG Timoshenko nanocomposites beam reinforced by a single-walled boron nitride nanotube. Saljooghi *et al.* (2014) analyzed free vibration of the FGB by reproducing the Kernel practical method. Khazal *et al.* (2016) assumed an extended element-free Galerkin method to study the FGMs. Hashemi *et al.* (2016) discussed the nonuniformity effect on free vibration analysis of FGB. Khan *et al.* (2016) offered a 1D finite element model that was used to analyze the free vibration of the FGB. Paul and Das (2016) studied the free vibration behavior of pre-stressed FGBs theoretically. Fouda *et al.* (2017) developed a modified porosity to analyze the free vibrations of a porous FGB. Kirs *et al.* (2018) used three numerical methods (Haar Wavelet Method, Finite Difference Method, and Differential Quadrature Method) for free vibration analysis of FGM beam. Alshorbagy *et al.* (2011) analyzed numerically the free vibration of the FGB with different material distribution by finite element method. Avcar and Alwan (2017) studied the free vibration of the Rayleigh beam composite of FG material. Ebrahimi and Barati (2018) presented the nonlocal couple stress theory to study the free vibration of FG nanobeams including the exact position of the neutral axis. Senthamarai Kannan and Ramesh (2019) studied the free vibration of the epoxy-carbon composite (I and channel) beam by mixing each of nanosilica and micro-sized carbon-terminated butadiene acrylonitrile copolymer (CTBN) rubber in an epoxy matrix. The hand lay-up method was used to fabricate a composite beam. Bouamama *et al.* (2018) studied the free vibration of sandwich FGB. Zhao *et al.* (2018) established a unified analytical model to study the performance of vibration of thick curved and straight FG porous beams with different boundary conditions. Ghadiri and Jafari (2018) studied the vibration of a cantilever nanobeam with FG material subjected to concentrated mass at a free end. Pradhan and Sarangi (2018) used the finite element method to analyze the free vibration of the FGB. Sayyad and Ghugal (2018) presented the exponential shear deformation theory to analyze the free vibration of FGBs with different conditions. Khazal *et al.* (2019) calculated the fracture parameters of the FGB by the technique of digital image. Nam *et al.* (2019) developed a new model of the beam based on modified FSDT to analyze the free vibration behavior of the variable thickness FGBs. Faeouq *et al.* (2019) examined the material properties of (epoxy and glass) FGM. AlSaid-Alwan and

Avcar (2020) employed Euler Bernoulli, Shear, Rayleigh, and Timoshenko beam theories to examine the free vibration of the FGB. Neamah *et al.* (2021) developed a new model of the FGB based on Euler and different Timoshenko beam theories to study buckling behavior, Neamah *et al.* (2022) presented analytical and numerical methods to simulate FGB. Avcar *et al.* (2021) used HSDT to analyze the frequency of sigmoid FG sandwich beams.

The objective of the present work is to derive and develop a new model of FGB depending on Euler, FSDT and HSDT. In this work, FGB was made from metal and ceramic materials, and their properties varied in the thickness direction according to the power-law distribution. Also, the influence of some parameters (modulus ratio, aspect ratio, power index value, and different beam theories methods) on the free vibration for this new model of the FGB are studied numerically and analytically. Dimensionless natural frequencies were presented analytically and numerically by using Fortran and Ansys APDL (17.2) respectively. This solution method and how to create this model with a high degree is based on Timoshenko's theories that were not presented in previous research.

MATERIAL AND METHODS

The FGB composed of ceramic and metal with a square cross-section was considered. The Cartesian coordinates (X-Z and Y) are taken along the length, height, and width of the beam as presented in Fig. 1.

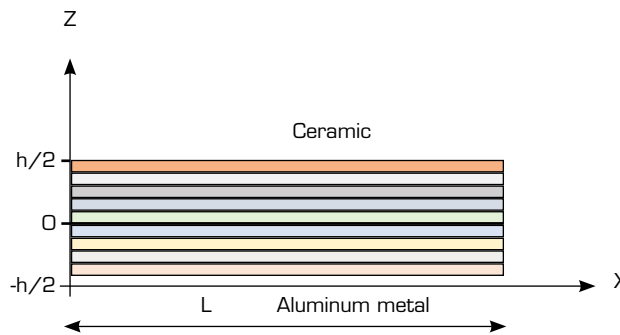


Figure 1. The geometry of FGB.

In this work, FGB consists of two dissimilar materials. The effective properties, i.e., density, Poisson's ratio, and modulus of elasticity (E) vary along the (z) direction according to the volume fraction function based on the rule of the mixture as shown in Eq. 1 (Şimşek and Yurtcu 2013):

$$P_{ef} = P_t V_t + P_b V_b \quad (1)$$

where P_t , P_b , V_t , V_b are the effective properties and volume fraction of the top and the bottom surface of FGB. The volume fraction is shown in Eq. 2:

$$V_t + V_b = 1 \quad (2)$$

In this study, the power-law distribution is used to describe the variation of material properties in a thickness direction. For upper material, the volume fraction is given by Eq. 3:

$$V_t = \left(\frac{z}{h} + \frac{1}{2} \right)^k \quad (3)$$

where K is the index value, that varies from 0 to infinity. The material variation profile through the thickness direction can be obtained depending on the value of this index. From the Eqs. 1, 2, and 3, the properties of FGB can be given as shown in Eq. 4:

$$P_Z = (P_t - P_b) \left(\frac{z}{h} + \frac{1}{2} \right)^k + P_b \quad (4)$$

The mathematical model is based on general beam deformation theories, the axial and transverse displacements U and W of any point of this beam are given in Eqs. 5–7 (Amara *et al.* 2016):

$$U(x, z, t) = u(x, t) - z \frac{\partial w}{\partial x} + f(z) \times u_1(x, t) \quad (5)$$

$$V(x, z, t) = 0 \quad (6)$$

$$W(x, z, t) = w(x, t) \quad (7)$$

where the axial and transverse displacements of any point on the neutral axis are (u and w) respectively, while (u_1) is a function that characterizes the effect of transverse shear strain on the middle surface of this FGB. Finally, $f(z)$ is the shape function that is used to find the distribution of transverse shear stress and strain over the thickness direction and they have the following forms in this work: in the CBT, $f(z) = 0$; in the FSDT, $f(z) = z$; in the HSDT, $f(z) = 4z^3/3h^2$ (Karamanli 2016).

From the values of the above shape functions, it can be seen that in the CBT (Euler's theorem) there is no transverse shear effect in the thickness direction, so the effect of transverse shear is neglected in this theory while this effect is taken in (FSDT and HSDT).

The normal and shear strains are given by Eqs. 8 and 9:

$$\varepsilon_{xx} = \frac{\partial u}{\partial x} - \left(z \frac{\partial^2 w}{\partial x^2} \right) + \left(f(z) \times \frac{\partial u_1}{\partial x} \right) \quad (8)$$

$$\gamma_{xz} = \frac{\partial U}{\partial z} + \frac{\partial W}{\partial x} = \left(\frac{\partial f}{\partial z} \times u_1 \right) \quad (9)$$

The motion equations will be found by applying Hamilton's principle (Eq. 10):

$$\int_{t_1}^{t_2} (\delta K - \delta U_{int} + \delta W_{ext}) dt = 0 \quad (10)$$

where t_1, t_2 are the initial and final times $\delta K, \delta U_{int}$ and δW_{ext} are the variation of kinetic energy, virtual strain energy and virtual external work respectively. The kinetic energy variation of this beam can be stated as shown in Eq. 11:

$$\begin{aligned} \delta K = \int \rho(z) \times [& \left(\left(\frac{\partial u}{\partial t} \right) - \left(z \times \frac{\partial}{\partial x} \left(\frac{\partial w}{\partial t} \right) \right) + \left(f(z) \times \left(\frac{\partial u_1}{\partial t} \right) \right) \right) \times \left(\delta \left(\frac{\partial u}{\partial t} \right) - \right. \\ & \left. \left(z \times \delta \frac{\partial}{\partial x} \left(\frac{\partial w}{\partial t} \right) \right) + \left(f(z) \times \delta \left(\frac{\partial u_1}{\partial t} \right) \right) \right) + \left(\left(\frac{\partial w}{\partial t} \right) \times \delta \left(\frac{\partial w}{\partial t} \right) \right)] dv = \int_0^l [\delta \left(\frac{\partial u}{\partial t} \right) \left((m_{00} \left(\frac{\partial u}{\partial t} \right) - \right. \right. \\ & \left. \left. (m_{11} \times \frac{\partial}{\partial x} \left(\frac{\partial w}{\partial t} \right) \right) + (m_f \times \left(\frac{\partial u_1}{\partial t} \right) \right)) + \delta \frac{\partial}{\partial x} \left(\frac{\partial w}{\partial t} \right) \left((-m_{11} \times \left(\frac{\partial u}{\partial t} \right) \right) + (m_{22} \times \frac{\partial}{\partial x} \left(\frac{\partial w}{\partial t} \right) - \right. \right. \\ & \left. \left. (m_{fz} \times \left(\frac{\partial u_1}{\partial t} \right) \right)) + \delta \left(\frac{\partial u_1}{\partial t} \right) \left((m_f \times \left(\frac{\partial u}{\partial t} \right) \right) - (m_{fz} \times \frac{\partial}{\partial x} \left(\frac{\partial w}{\partial t} \right) \right) + (m_{f^2} \times \left(\frac{\partial u_1}{\partial t} \right)) \right) + \right. \\ & \left. \left(\delta \left(\frac{\partial w}{\partial t} \right) \times \left(\frac{\partial w}{\partial t} \right) \right)] dx \end{aligned} \quad (11)$$

where $\rho(z)$ is the mass density, and $(m_{00}, m_{11}, m_{22}, m_p, m_{fz}, m_{z^2})$ are the mass inertias and defined as: $\int \rho(z) \times (1, z, z^2, f(z), z \times f(z), f(z)^2) dA$, respectively.

The variation of strain energy of the beam can be defined as in Eq. 12:

$$\begin{aligned} \delta(U_{int}) = \int [(\sigma_{xx} \times \delta\varepsilon_{xx}) + (\sigma_{xz} \times \delta\gamma_{xz})] dV = \int [\sigma_{xx} \times (\delta \frac{du}{dx} - z \delta \frac{d^2w}{dx^2} + f(z) \delta \frac{du_1}{dx}) \\ + \sigma_{xz} \times (\frac{df(z)}{dz} \times \delta u_1)] dV = \int_0^l [N \times \delta \frac{du}{dx} - M \times \delta \frac{d^2w}{dx^2} + M^s \times \delta \frac{du_1}{dx} + Q^s \times \delta u_1] dx \end{aligned} \quad (12)$$

where N , M , M^s , and Q^s are the stress resultants calculated in Eqs. 13–19:

$$N = \int \sigma_{xx} dA \quad (13)$$

$$M = \int z \times \sigma_{xx} dA \quad (14)$$

$$M^s = \int f(z) \times \sigma_{xx} dA \quad (15)$$

$$Q^s = \int \frac{df(z)}{dz} \sigma_{xz} \times K_s dA \quad (16)$$

$$\sigma_{xx} = E(z) \times \varepsilon_{xx} \quad (17)$$

$$\sigma_{xz} = G(z) \times \gamma_{xz} \quad (18)$$

$$G(z) = E(z) / 2(1+\nu) \quad (19)$$

By substituting the Eqs. 8 and 9 in the Eqs. 17 and 18 and then substituting the results in Eqs. 13 to 15, and Eq. 16, the stress resultants are obtained in Eqs. 20–23:

$$N = A_{11} \times \frac{du}{dx} - B_{11} \times \frac{d^2w}{dx^2} + E_{11} \times \frac{du_1}{dx} \quad (20)$$

$$M = B_{11} \times \frac{du}{dx} - D_{11} \times \frac{d^2w}{dx^2} + F_{11} \times \frac{du_1}{dx} \quad (21)$$

$$M^s = E_{11} \times \frac{du}{dx} - F_{11} \times \frac{d^2w}{dx^2} + H_{11} \times \frac{du_1}{dx} \quad (22)$$

$$Q^s = A_{55} \times u_1 \times K_s \quad (23)$$

where:

$$(A_{11}, B_{11}, D_{11}, E_{11}, F_{11}, H_{11}) = \int E(z) \times (1, z, z^2, f(z), zf(z), (f(z))^2) dA \quad (24)$$

$$A_{55} = \int G(z) \times \frac{df(z)^2}{dx^2} dA \quad (25)$$

The variation of external work by the applied transverse load q can be written as in Eq. 26:

$$\delta(W_{ext}) = \int_0^l (q \times \delta w) dx = 0 \quad (26)$$

This is due to fact in free vibration there is no external work.

By substituting the expression of δK , δU_{int} , and δW_{ext} in Eq. 10 the Eq. 27 is given:

$$\begin{aligned} \int_{t_1}^{t_2} \int_0^l \left[\delta \left(\frac{\partial u}{\partial t} \right) \left(m_{00} \left(\frac{\partial u}{\partial t} \right) \right) - \left(m_{11} \times \frac{\partial}{\partial x} \left(\frac{\partial w}{\partial t} \right) \right) + \left(m_f \times \left(\frac{\partial u_1}{\partial t} \right) \right) \right] + \delta \frac{\partial}{\partial x} \left(\frac{\partial w}{\partial t} \right) \left(-m_{11} \times \left(\frac{\partial u}{\partial t} \right) \right) + \\ \left(m_{22} \times \frac{\partial}{\partial x} \left(\frac{\partial w}{\partial t} \right) \right) - \left(m_{fz} \times \left(\frac{\partial u_1}{\partial t} \right) \right) + \delta \left(\frac{\partial u_1}{\partial t} \right) \left(m_f \times \left(\frac{\partial u}{\partial t} \right) \right) - \left(m_{fz} \times \frac{\partial}{\partial x} \left(\frac{\partial w}{\partial t} \right) \right) + \\ \left(m_{fz} \times \left(\frac{\partial u_1}{\partial t} \right) \right) + \left(m_{00} \times \delta \left(\frac{\partial w}{\partial t} \right) \times \left(\frac{\partial w}{\partial t} \right) \right) - \left(N \times \delta \frac{du}{dx} - M \frac{d^2 w}{dx^2} + M^s \times \delta \frac{du_1}{dx} + Q^s \times \delta u_1 \right) dx dt = 0 \end{aligned} \quad (27)$$

By integration by part and putting the coefficient (δu , δw , and δu_1) equal to zero, Eqs. 28–30 can be found:

$$\left(\frac{dN}{dx} \right) = \left(m_{00} \left(\frac{\partial^2 u}{\partial t^2} \right) \right) - \left(m_{11} \times \frac{\partial}{\partial x} \left(\frac{\partial^2 w}{\partial t^2} \right) \right) + \left(m_f \times \left(\frac{\partial^2 u_1}{\partial t^2} \right) \right) \quad (28)$$

$$\left(\frac{d^2 M}{dx^2} \right) = \left(m_{11} \times \frac{\partial}{\partial x} \left(\frac{\partial^2 u}{\partial t^2} \right) \right) - \left(m_{22} \times \frac{\partial^2}{\partial x^2} \left(\frac{\partial^2 w}{\partial t^2} \right) \right) + \left(m_{fz} \times \frac{\partial}{\partial x} \left(\frac{\partial^2 u_1}{\partial t^2} \right) \right) + \left(m_{00} \times \left(\frac{\partial^2 w}{\partial t^2} \right) \right) \quad (29)$$

$$- \left(\frac{dM^s}{dx} - Q^s \right) = \left(m_f \times \left(\frac{\partial^2 u}{\partial t^2} \right) \right) - \left(m_{fz} \times \frac{\partial}{\partial x} \left(\frac{\partial^2 w}{\partial t^2} \right) \right) + \left(m_{fz} \times \left(\frac{\partial^2 u_1}{\partial t^2} \right) \right) \quad (30)$$

From Eqs. 20–23 and 28–30, Eqs. 31–33 can be found:

$$\begin{aligned} \left(A_{11} \times \frac{d^2 u}{dx^2} \right) - \left(B_{11} \times \frac{d^3 w}{dx^3} \right) + \left(E_{11} \times \frac{d^2 u_1}{dx^2} \right) = \left(m_{00} \left(\frac{\partial^2 u}{\partial t^2} \right) \right) - \left(m_{11} \times \frac{\partial}{\partial x} \left(\frac{\partial^2 w}{\partial t^2} \right) \right) + \\ \left(m_f \times \left(\frac{\partial^2 u_1}{\partial t^2} \right) \right) \end{aligned} \quad (31)$$

$$\begin{aligned} \left(B_{11} \times \frac{d^3 u}{dx^3} \right) - \left(D_{11} \times \frac{d^4 w}{dx^4} \right) + \left(F_{11} \times \frac{d^3 u_1}{dx^3} \right) = \left(m_{11} \times \frac{\partial}{\partial x} \left(\frac{\partial^2 u}{\partial t^2} \right) \right) - \\ \left(m_{22} \times \frac{\partial^2}{\partial x^2} \left(\frac{\partial^2 w}{\partial t^2} \right) \right) + \left(m_{fz} \times \frac{\partial}{\partial x} \left(\frac{\partial^2 u_1}{\partial t^2} \right) \right) + \left(m_{00} \times \left(\frac{\partial^2 w}{\partial t^2} \right) \right) \end{aligned} \quad (32)$$

$$(E_{11} \times \frac{d^2 u}{dx^2}) - (F_{11} \times \frac{d^3 w}{dx^3}) + (H_{11} \times \frac{d^2 u_1}{dx^2}) - (A_{55} \times u_1) = \left(m_f \times \left(\frac{\partial^2 u}{\partial t^2} \right) \right) - \left(m_{fz} \times \frac{\partial}{\partial x} \left(\frac{\partial^2 w}{\partial t^2} \right) \right) + \left(m_{f^2} \times \left(\frac{\partial^2 u_1}{\partial t^2} \right) \right) \quad (33)$$

Analytical Solution for Free Vibration

For the free vibration in s-s FGB, the above motion equations are solved analytically by using the procedure of Navier's solution. The functions of displacement are uttered as the product of trigonometric function to satisfy the motion equations, the fields of displacements are presented as Eqs. 34–36 (Rahmani and Pedram 2014):

$$u(x, t) = \sum_{n=1}^N U_n \times \cos(\alpha x) \times e^{i\omega_n t} \quad (34)$$

$$w(x, t) = \sum_{n=1}^N w_n \times \sin(\alpha x) \times e^{i\omega_n t} \quad (35)$$

$$u_1(x, t) = \sum_{n=1}^N G_n \times \cos(\alpha x) \times e^{i\omega_n t} \quad (36)$$

Based on FSDT, HSDT and by substituting the Eqs. 34 to 36 and their derivatives into the equation of motion (31–33), the analytical solution can be found as follows (Eq. 37):

$$\begin{pmatrix} (-\alpha^2 \times A_{11}) & (\alpha^3 \times B_{11}) & (-\alpha^2 \times E_{11}) \\ (\alpha^3 \times B_{11}) & (-\alpha^4 \times D_{11}) & (F_{11} \times \alpha^3) \\ (-\alpha^2 \times E_{11}) & (F_{11} \times \alpha^3) & (-\alpha^2 \times H_{11} - A_{55} \times K_s) \end{pmatrix} - \omega_n^2 \begin{pmatrix} m_{00} & -\alpha \times m_{11} & m_f \\ -\alpha \times m_{11} & m_{22} \times \alpha^2 + m_{00} & -m_{fz} \times \alpha \\ m_f & -m_{fz} \times \alpha & m_{f^2} \end{pmatrix} \begin{bmatrix} U_n \\ W_n \\ G_n \end{bmatrix} = \begin{bmatrix} 0 \\ 0 \\ 0 \end{bmatrix} \quad (37)$$

By using the CBT, the values of G_n and $(H_{11}, F_{11}, E_{11}, M_P, M_{F2}, E_{FZ})$ are equal to zero. The analytical solution can be found in Eq. 38:

$$\begin{bmatrix} (-\alpha^2 \times A_{11}) & (\alpha^3 \times B_{11}) \\ (\alpha^3 \times B_{11}) & (-\alpha^4 \times D_{11} + \alpha^2 \times P) \end{bmatrix} - \omega_n^2 \begin{bmatrix} m_{00} & -m_{11} \times \alpha \\ -m_{11} \times \alpha & m_{22} \times \alpha^2 \end{bmatrix} \begin{bmatrix} U_n \\ W_n \end{bmatrix} = \begin{bmatrix} 0 \\ 0 \end{bmatrix} \quad (38)$$

The values of natural frequency by using the CBT, FSDT, and HSDT were calculated analytically in the Fortran program.

Numerical Modeling

In Ansys APDL (17.2) software, a 2D model for this type of FGB was built to simulate and analyze the free vibration problems. In this section, the FGB has consisted of 10 layers through the thickness direction. The material properties (modulus of elasticity, density, and poisons ratio) of each layer are completely different from the other and not constant, which vary according to the power's law form and calculated in each FGB layer by using the Excel program then entered manually to Ansys software. In the meshing stage, the shell element (shell 281) was used due to its features. The FGB was modeled by drawing the length and width while the thickness was represented from 10 layers, each one with the same thickness. The number of elements and nodes depends on the convergence criteria of numerical solutions and FGB length is (2600–8600) elements and (6380–25500) nodes. The extrude option has been selected to illustrate the 10 layers that create the FGB thickness (Fig. 2).

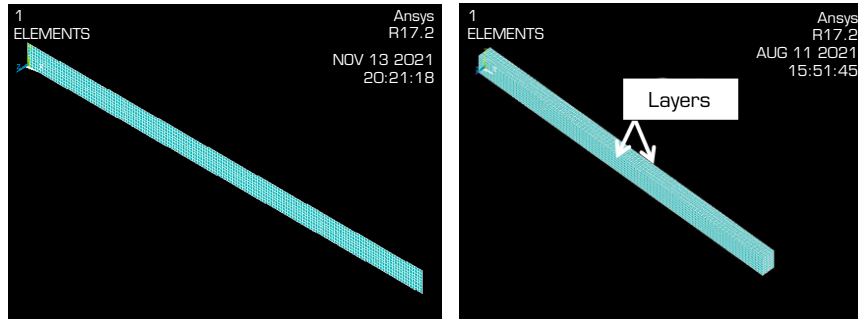


Figure 2. Mesh of 1 and 10 layers of FGB.

RESULTS AND DISCUSSION

In the present work, a new model of s-s FGB has been derived based on different beam theories to calculate the free vibration. The effect of various parameters on natural frequency was investigated numerically and analytically.

To prove the accuracy of the developed mathematical and numerical model in predicting the natural frequencies of the FGB, this model of simply supporting FGB was built with 0.4 widths and 20 lengths. The material properties (Marzoq and Al-Ansari 2021; Şimşek and Kocatürk 2009) were presented in Table 1.

Table 1. The material properties used.

Property	Steel	Al ₂ O ₃
Modulus of elasticity (E) GPas	210	390
Poison ratio (ν)	0.3	0.3
Density (ρ) kg·m ⁻³	7800	3960

Source: Marzoq and Al-Ansari (2021) and Şimşek and Kocatürk (2009).

The dimensionless natural frequency of FGB for different modulus ratio (ER), aspect ratio (L/H) and power index value (K) were given by Eq. 39 (Marzoq and Al-Ansari 2021; Şimşek and Kocatürk 2009).

$$\lambda^2 = \omega L^2 \sqrt{\frac{\rho_m A}{E_m I}} \quad (39)$$

where: (λ , ω , I , and A) are the dimensionless frequency, frequency in (rad/s), FGB the moment of inertia and cross section area of this beam were calculated as Eq. 40:

$$I = \frac{bh^3}{12} \quad (40)$$

Tables 2 and 3 showed the comparison among the dimensionless natural frequency of the present work and that of Marzoq and Al-Ansari (2021) and Şimşek and Kocatürk (2009) for s-s FGB, with aspect ratio values of 20 and 100 and modulus ratios (ER) of 0.25, 0.5, 1, 2 and 4.

Table 2. Validation of dimension less natural frequency for s-s FGB when L/H = 20.

ER	Author	Index						
		0.1	0.2	0.5	1	2	5	10
0.25	Present Ansys – Shell Model	2.3374	2.414	2.571	2.715	2.846	2.947	3.005
	Present CBT	2.3733	2.460	2.596	2.702	2.804	2.928	3.006
	Present FSDT	2.3697	2.456	2.592	2.698	2.800	2.924	3.002
	Present HSDT	2.3726	2.459	2.595	2.701	2.803	2.927	3.006
	Marzoq and Al-Ansari (2021)	2.1571	2.232	2.386	2.528	2.657	2.765	2.802
	Şimşek and Kocatürk (2009)	2.3739	2.460	-	2.703	2.805	-	3.008
0.5	Present Ansys – Shell Model	2.6526	2.689	2.770	2.850	2.927	3.005	3.029
	Present CBT	2.7093	2.756	2.834	2.893	2.944	3.009	3.054
	Present FSDT	2.7052	2.751	2.830	2.888	2.940	3.005	3.050
	Present HSDT	2.7085	2.755	2.833	2.892	2.943	3.008	3.053
	Marzoq and Al-Ansari (2021)	2.4544	2.489	2.567	2.647	2.724	2.792	2.816
	Şimşek and Kocatürk (2009)	2.7104	2.757	-	2.894	2.945	-	3.056
1	Present Ansys – Shell Model	3.0669	3.066	3.066	3.066	3.066	3.066	3.066
	Present CBT	3.1383	3.138	3.138	3.138	3.138	3.138	3.138
	Present FSDT	3.1336	3.133	3.133	3.133	3.133	3.133	3.133
	Present HSDT	3.1374	3.137	3.137	3.137	3.137	3.137	3.137
	Marzoq and Al-Ansari (2021)	2.8442	2.844	2.844	2.844	2.844	2.844	2.844
	Şimşek and Kocatürk (2009)	3.1399	3.139	3.139	3.139	3.139	3.139	3.139
2	Present Ansys – Shell Model	3.589	3.558	3.479	3.389	3.289	3.182	3.135
	Present CBT	3.675	3.628	3.527	3.440	3.374	3.317	3.270
	Present FSDT	3.6699	3.622	3.522	3.435	3.369	3.312	3.265
	Present HSDT	3.6742	3.627	3.526	3.439	3.373	3.316	3.269
	Marzoq and Al-Ansari (2021)	3.335	3.306	3.233	3.146	3.045	2.936	2.894
	Şimşek and Kocatürk (2009)	3.6775	3.630	-	3.442	3.376	-	3.272
4	Present Ansys – Shell Model	4.2329	4.174	4.023	3.840	3.620	3.370	3.251
	Present CBT	4.3344	4.243	4.0324	3.821	3.647	3.530	3.4529
	Present FSDT	4.3280	4.237	4.0269	3.816	3.642	3.524	3.447
	Present HSDT	4.3331	4.242	4.0312	3.820	3.646	3.529	3.4519
	(Marzoq and Al-Ansari 2021)	3.9361	3.882	3.745	3.572	3.353	3.089	2.981
	(Şimşek and Kocatürk 2009)	4.337	4.245	-	3.823	3.648	-	3.454

Table 3. Validation of dimension less natural frequency for s-s FGB when L/H = 100.

ER	Author	Index						
		0.1	0.2	0.5	1	2	5	10
0.25	Present Ansys Shell Model	2.482	2.546	2.6717	2.775	2.861	2.952	3.0108
	Present CBT	2.374	2.461	2.5980	2.703	2.805	2.930	3.008
	Present FSDT	2.374	2.461	2.5976	2.703	2.805	2.930	3.008
	Present HSDT	2.373	2.460	2.5976	2.703	2.805	2.930	3.008
	Marzoq and Al-Ansari (2021)	2.504	2.569	2.6976	2.805	2.898	2.995	3.053
	Şimşek and Kocatürk (2009)	2.375	2.462	-	2.705	2.807	-	3.01
0.5	Present Ansys Shell Model	2.758	2.791	2.8593	2.917	2.966	3.020	3.056
	Present CBT	2.710	2.757	2.8361	2.894	2.946	3.010	3.056
	Present FSDT	2.710	2.757	2.8360	2.894	2.945	3.010	3.056
	Present HSDT	2.710	2.757	2.8362	2.894	2.946	3.010	3.056
	Marzoq and Al-Ansari (2021)	2.776	2.810	2.8782	2.937	2.989	3.044	3.080
	Şimşek and Kocatürk (2009)	2.711	2.758	-	2.896	2.947	-	3.057
1	Present Ansys Shell Model	3.140	3.140	3.1405	3.140	3.140	3.140	3.140
	Present CBT	3.140	3.140	3.1400	3.140	3.140	3.140	3.140
	Present FSDT	3.139	3.139	3.1397	3.139	3.139	3.139	3.139
	Present HSDT	3.139	3.139	3.1398	3.139	3.139	3.139	3.139
	Marzoq and Al-Ansari (2021)	3.163	3.163	3.1632	3.163	3.163	3.163	3.163
	Şimşek and Kocatürk (2009)	3.141	3.141	3.1415	3.141	3.141	3.141	3.141
2	Present Ansys Shell Model	3.640	3.608	3.5381	3.469	3.407	3.339	3.287
	Present CBT	3.677	3.629	3.5298	3.442	3.376	3.319	3.272
	Present FSDT	3.676	3.629	3.5293	3.442	3.376	3.319	3.272
	Present HSDT	3.676	3.629	3.5292	3.442	3.376	3.319	3.272
	Marzoq and Al-Ansari (2021)	3.679	3.636	3.5644	3.493	3.456	3.383	3.332
	Şimşek and Kocatürk (2009)	3.679	3.632	-	3.444	3.378	-	3.274
4	Present Ansys Shell Model	4.268	4.208	4.0693	3.924	3.787	3.637	3.523
	Present CBT	4.336	4.245	4.0345	3.823	3.649	3.532	3.454
	Present FSDT	4.336	4.245	4.0342	3.823	3.649	3.532	3.454
	Present HSDT	4.335	4.244	4.0338	3.823	3.648	3.532	3.454
	Marzoq and Al-Ansari (2021)	4.345	4.284	4.1394	3.984	3.831	3.669	3.557
	Şimşek and Kocatürk (2009)	4.339	4.248	-	3.825	3.651	-	3.456

The present analytical models are compatible with Marzoq and Al-Ansari (2021) and Şimşek and Kocatürk (2009). From the previous comparisons, the numerical and analytical developed models with several kinds of research give an excellent agreement.

In the current work, the free vibration analysis for a simple supported FGB is presented analytically and numerically by using Fortran and Ansys programs. The influence of several parameters such as aspect ratio (length to thickness ratio = L/H), modulus ratio (E ratio = E_t/E_b), power index value (K), and theories of deformation (CBT, FSDT, HSDT, and Ansys) on dimensionless natural frequency have been studied and discussed.

To investigate the effect of aspect ratio, five values ($L/H = 5, 10, 20, 50,$ and 100) are studied analytically and numerically. Figures 3–7 show the first mode of some FGB models that have been built in Ansys (12.7) APDL software. From the nodal solution, the maximum value of frequency is inserted in the Eq. 39 to calculate the maximum dimensionless frequency. Figs. 8–12, 13–17, 18–22, and 23–27 show the relationship between the dimensionless natural frequency and power index value with different aspect ratios and beam deformation theories (CBT, FSDT, HSDT, and Ansys).

It can be determined from these figures for CBT the parameter of aspect ratio not influenced the dimensionless natural frequency due to neglecting the effect of shear, while there is a significant influence of this ratio on TBT and HSDT. Generally, the dimensionless natural frequency increases when this parameter increases at the same value for the modulus ratio. This is because the dimensionless frequency is directly proportional to the length to thickness ratio (aspect ratio), as shown in Eq. 39. In addition, the numerical results from the Ansys program are similar to that of TBT.

Figures 28–35 illustrate the effect of modulus ratio ($E_t/E_b = ER = 0.25, 0.333, 0.5, 0.75, 1, 1.333, 2, 3$ and 4) and power index value ($K = 0, 0.1, 0.2, 0.4, 0.6, 0.8, 1, 5, 10, 20, 30, 50$ and 10000) on dimensionless frequency of the FGB when the value of aspect ratio is 5 numerically and analytically. From these figures, it may be concluded that when the E ratio increases, the dimensionless frequency decreases. If E ratio < 1 , the modulus of the bottom material is larger than the top one and an increase in power index value leads to an increase in equivalent elastic modulus of this beam, as shown in Eq. 4. This increase leads to an increase in the dimensionless frequency. Also, if E ratio > 1 , the modulus of the bottom material is smaller than that one in the top, any increase in power index value will reduce the equivalent elastic modulus of this beam and lead to a decrease in the dimensionless natural frequency. In this case, when the power index value is equal to infinity, the pure metal will give us the lowest value of frequency, on the other hand, if the power index value is zero, the pure ceramic will give a higher value. From the same figures, the effect of index value on the dimensionless natural frequency can be observed at different E ratios for four developed models. From these figures, it can be concluded that, when the power index value remains constant and the E ratio increases, the dimensionless frequency will increase.

Figures 36–44 illustrate the deformation theory's effect on the dimensionless natural frequency of FGB with 5 aspect ratio and different values of power index and the modulus ratio. These figures show that the dimensionless frequency of CBT is greater than that of TBT and HSDT beam theories as well from the Ansys program. That means the including of shear's effectiveness leads to minimizing the dimensionless natural frequency.

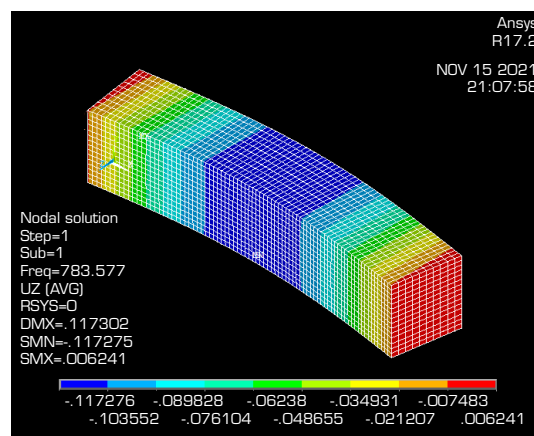


Figure 3. The first mode shape of simply supported FGB at L/h 5.

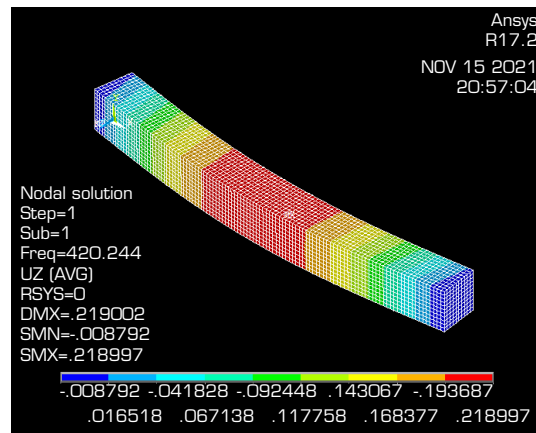


Figure 4. The first mode shape of simply supported FGB at L/h 10.

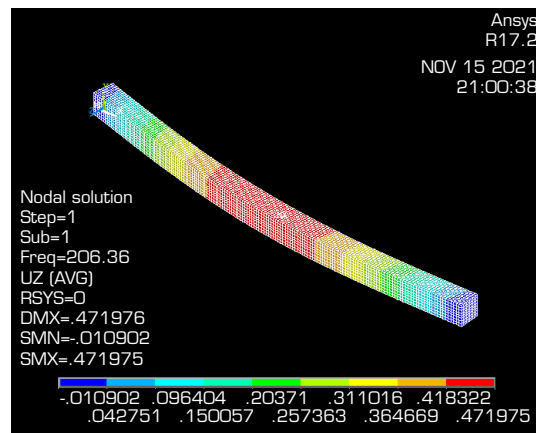


Figure 5. The first mode shape of simply supported FGB at L/h 20.

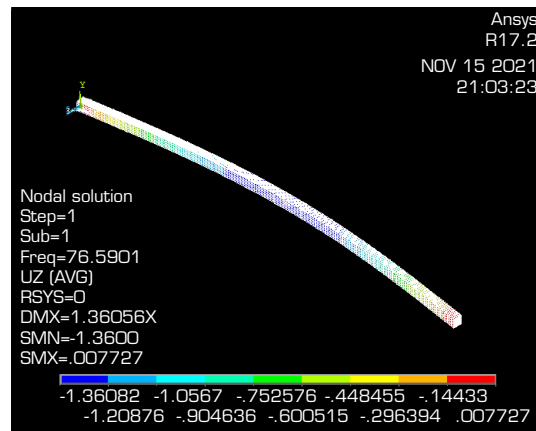


Figure 6. The first mode shape of simply supported FGB at L/h 50.

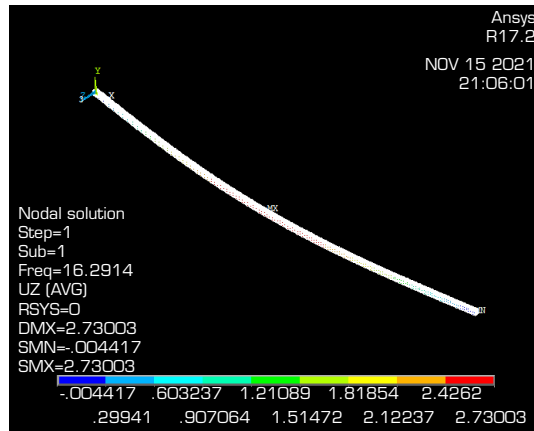


Figure 7. The first mode shape of simply supported FGB at L/h 100.

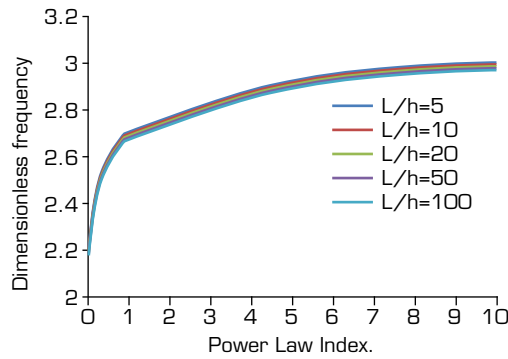


Figure 8. Dimensionless frequency of FGB when E ratio = 0.25 by CBT.

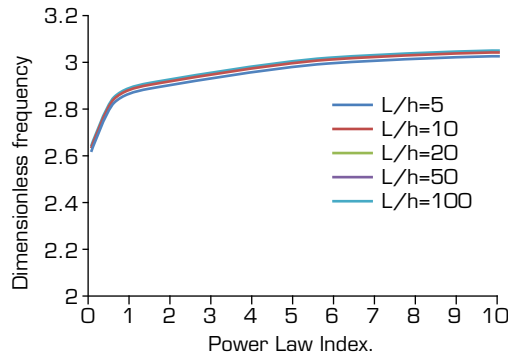


Figure 9. Dimensionless frequency of FGB when E ratio=0.5 by CBT.

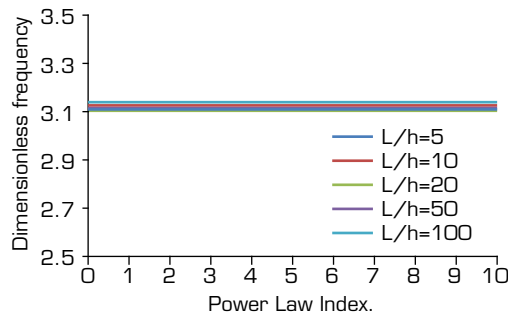


Figure 10. Dimensionless frequency of FGB when E ratio = 1 by CBT.

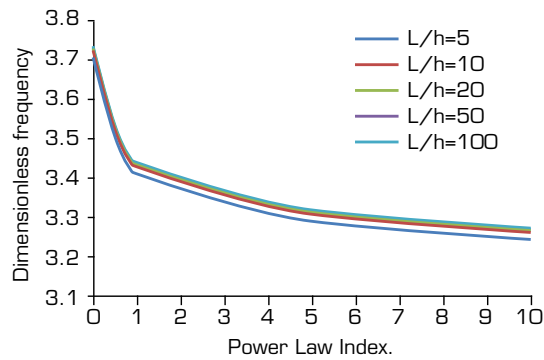


Figure 11. Dimensionless frequency of FGB when E ratio = 2 by CBT.

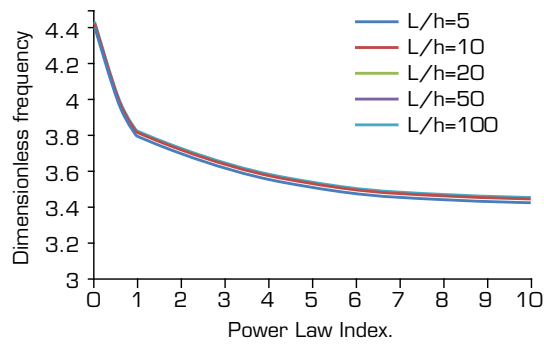


Figure 12. Dimensionless frequency of FGB when E ratio = 4 by CBT.

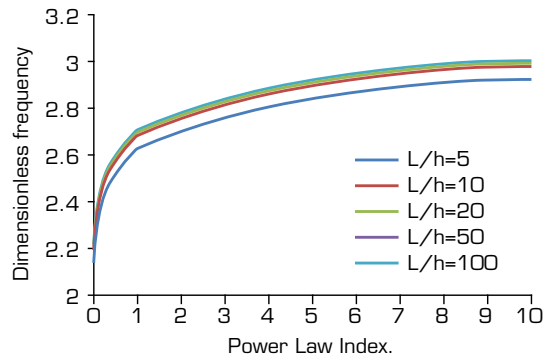


Figure 13. Dimensionless frequency of FGB when E ratio = 0.25 by FSDT.

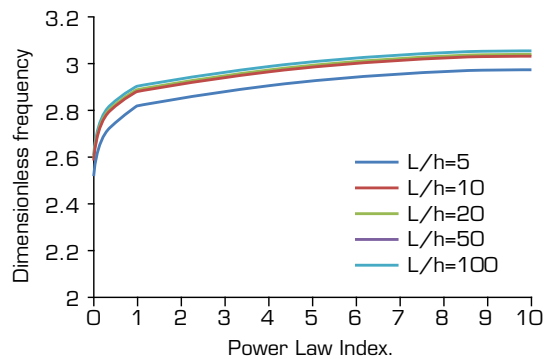


Figure 14. Dimensionless frequency of FGB when E ratio = 0.5 by FSDT.

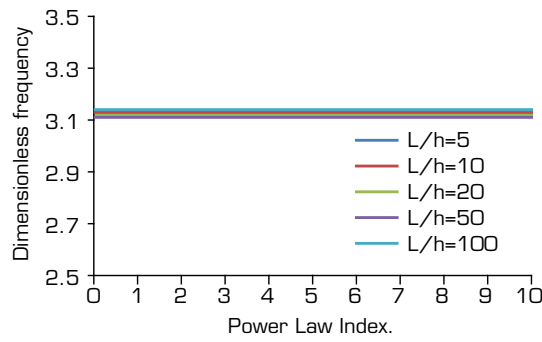


Figure 15. Dimensionless frequency of FGB when E ratio = 1 by FSDT.

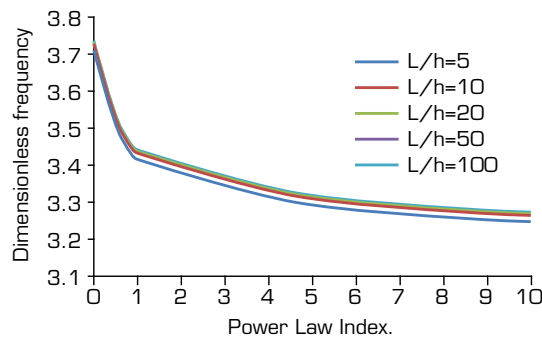


Figure 16. Dimensionless frequency of FGB when E ratio = 2 by FSDT.

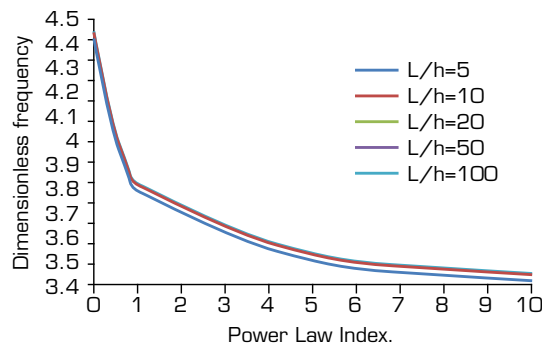


Figure 17. Dimensionless frequency of FGB when E ratio = 4 by FSDT.

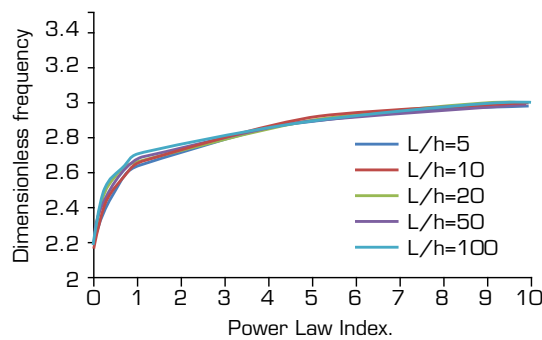


Figure 18. Dimensionless frequency of FGB when E ratio = 0.25 by HSDT.

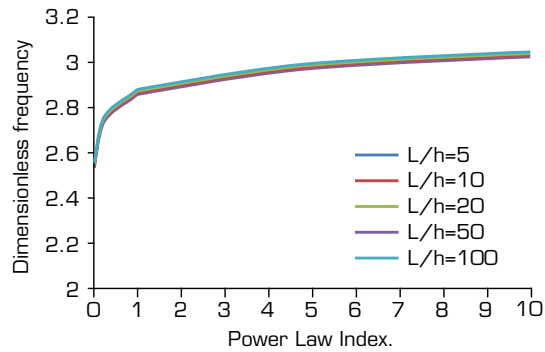


Figure 19. Dimensionless frequency of FGB when E ratio = 0.5 by HSDT.

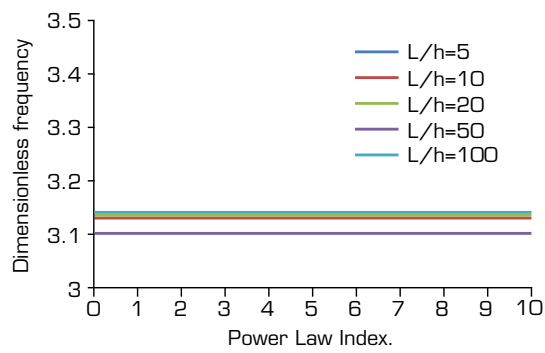


Figure 20. Dimensionless frequency of FGB when E ratio = 1 by HSDT.

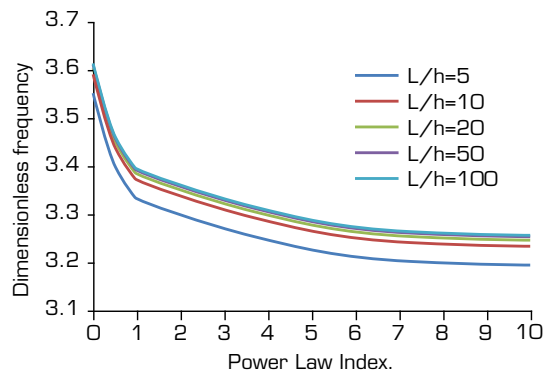


Figure 21. Dimensionless frequency of FGB when E ratio = 2 by HSDT.

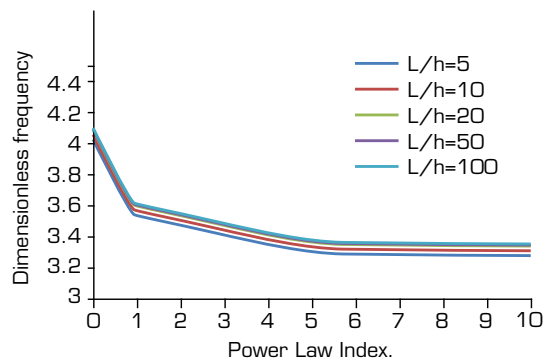


Figure 22. Dimensionless frequency of FGB when E ratio = 4 by HSDT.

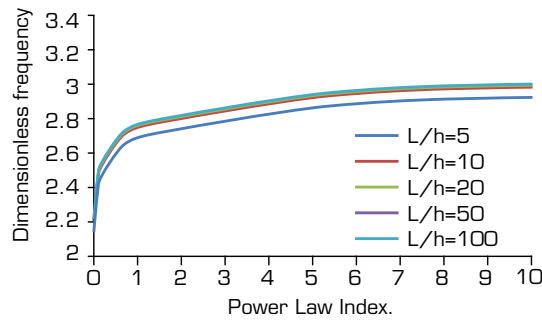


Figure 23. Dimensionless frequency of FGB when E ratio = 0.25 by Ansys.

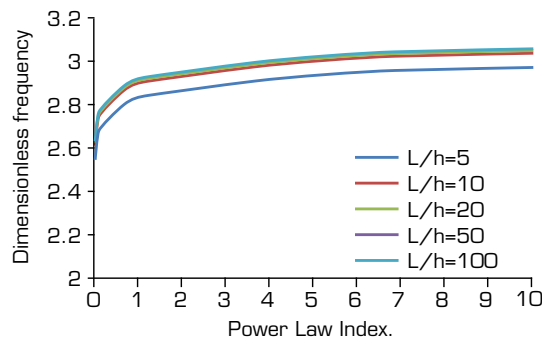


Figure 24. Dimensionless frequency of FGB when E ratio = 0.5 by Ansys.

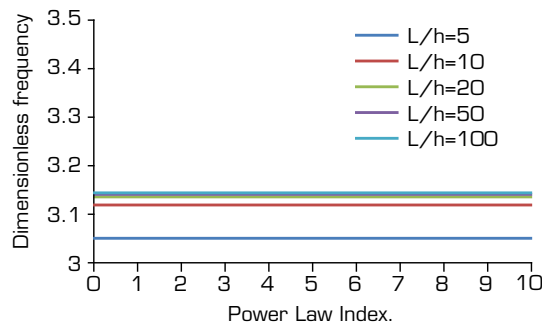


Figure 25. Dimensionless frequency of FGB when E ratio = 1 by Ansys.

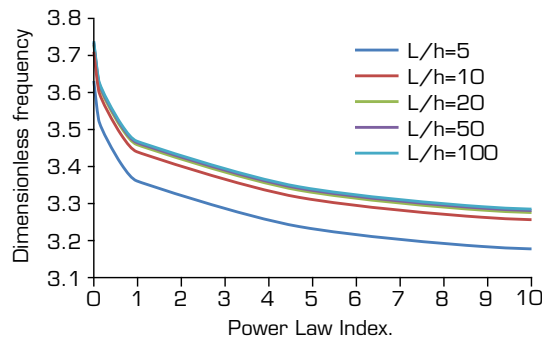


Figure 26. Dimensionless frequency of FGB when E ratio = 2 by Ansys.

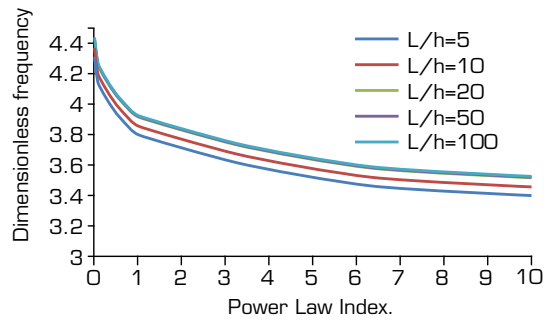


Figure 27. Dimensionless frequency of FGB when E ratio = 4 by Ansys.

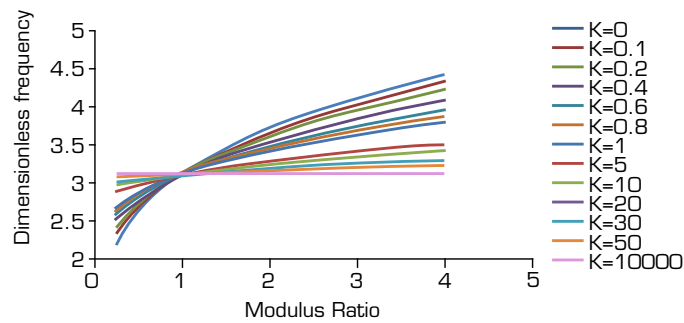


Figure 28. Dimensionless frequency of FGB when L/h = 5 by CBT.

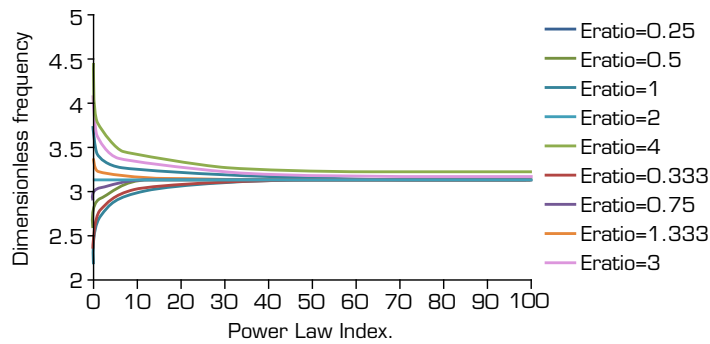


Figure 29. Dimensionless frequency of FGB when L/h = 5 by CBT.

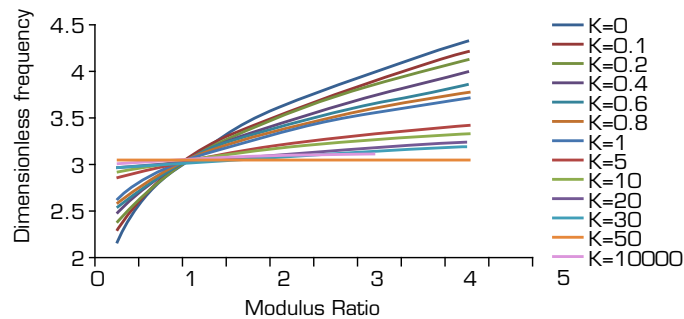


Figure 30. Dimensionless frequency of FGB when L/h = 5 by FSDT.

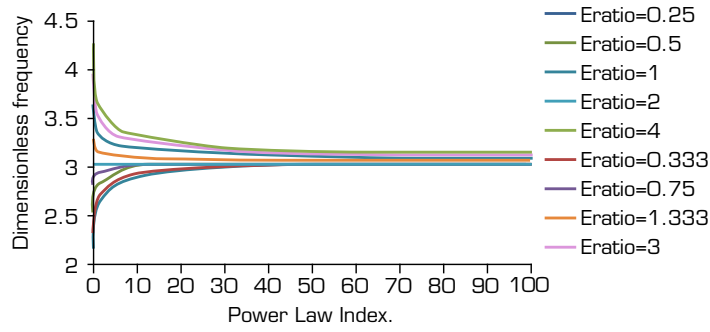


Figure 31. Dimensionless frequency of FGB when $L/h = 5$ by FSDT.

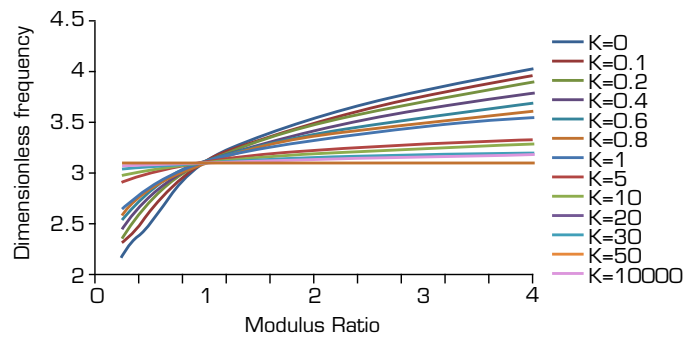


Figure 32. Dimensionless frequency of FGB when $L/h = 5$ by HSDT.

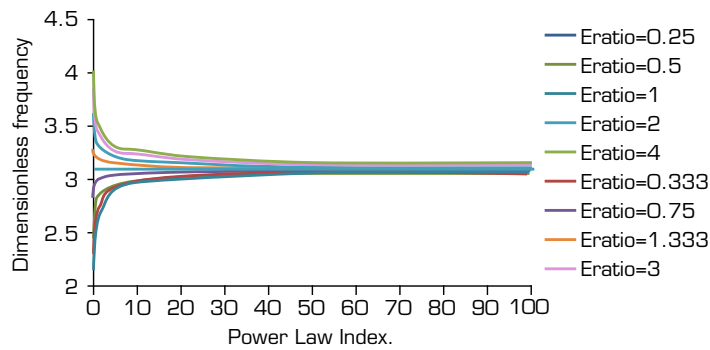


Figure 33. Dimensionless frequency of FGB when $L/h = 5$ by HSDT.

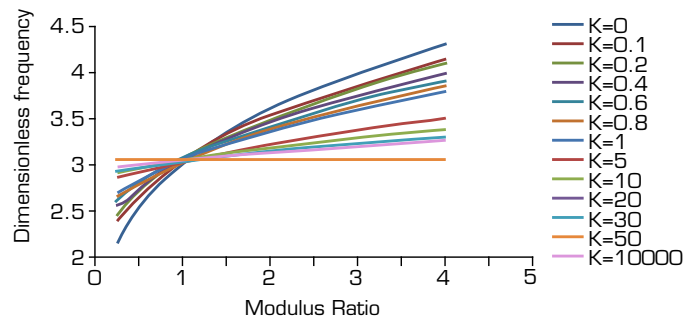


Figure 34. Dimensionless frequency of FGB when $L/h = 5$ by Ansys.

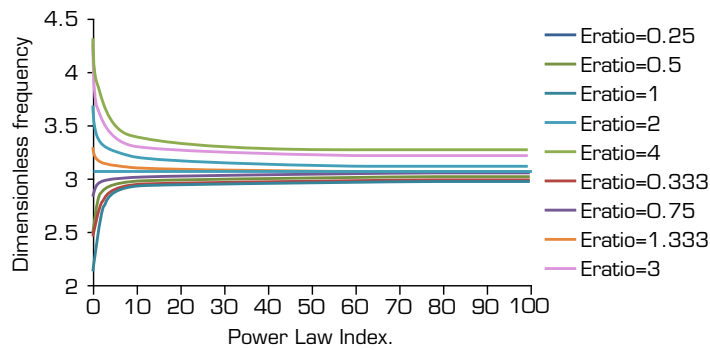


Figure 35. Dimensionless frequency of FGB when $L/h = 5$ by Ansys.

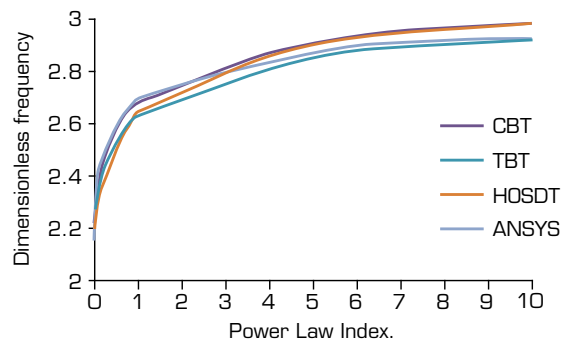


Figure 36. Dimensionless frequency of FGB when $L/h = 5$ and E ratio = 0.25 for all theories.

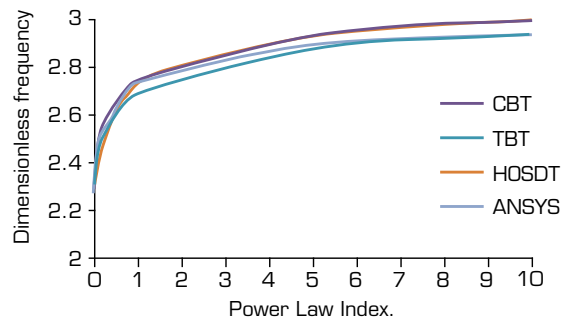


Figure 37. Dimensionless frequency of FGB when $L/h = 5$ and E ratio = 0.333 for all theories.

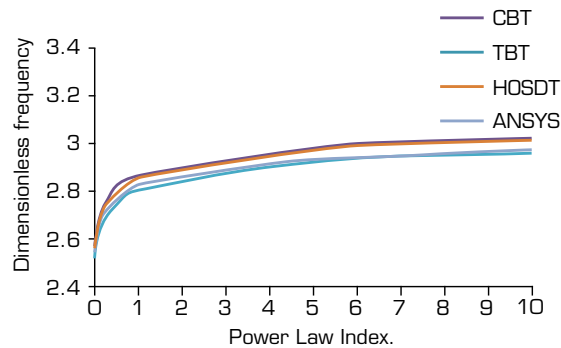


Figure 38. Dimensionless frequency of FGB when $L/h = 5$ and E ratio = 0.5 for all theories.

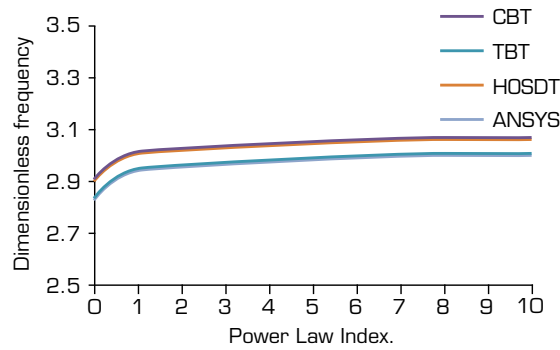


Figure 39. Dimensionless frequency of FGB when $L/h = 5$ and E ratio = 0.75 for all theories.

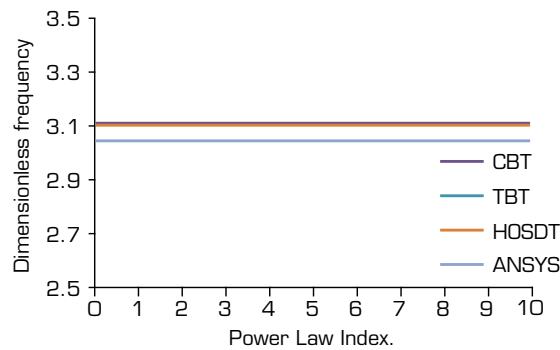


Figure 40. Dimensionless frequency of FGB when $L/h = 5$ and E ratio = 1 for all theories.

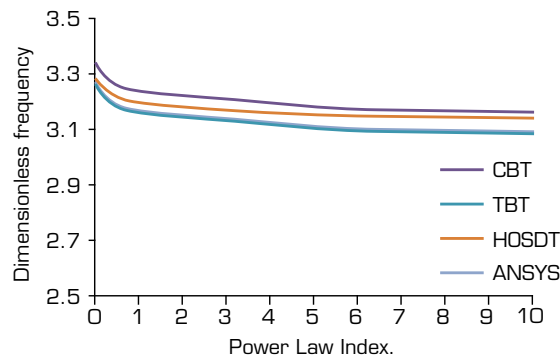


Figure 41. Dimensionless frequency of FGB when $L/h = 5$, E ratio = 1.333 for all theories.

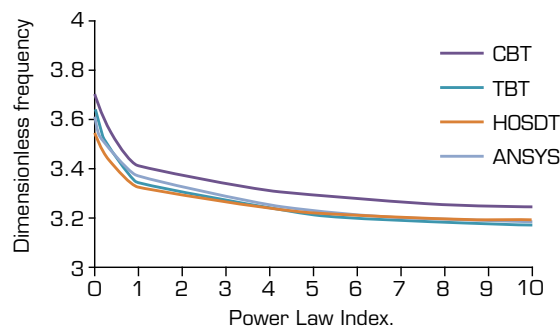


Figure 42. Dimensionless frequency of FGB when $L/h = 5$, E ratio = 2 for all theories.

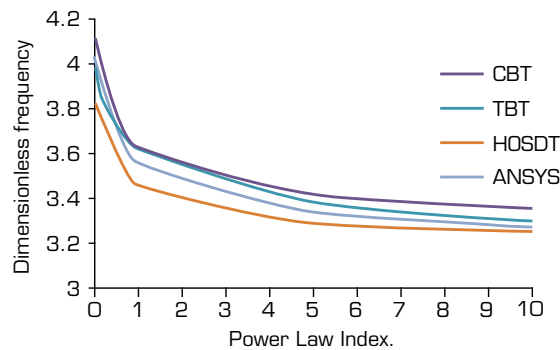


Figure 43. Dimensionless frequency of FGB when $L/h = 5$, E ratio = 3 for all theories.

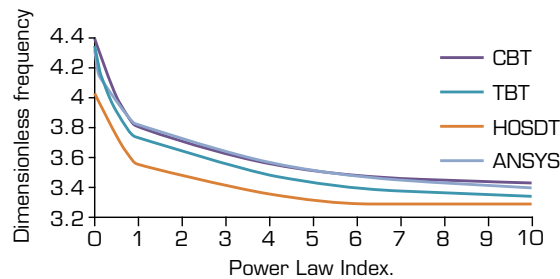


Figure 44. Dimensionless frequency of FGB when $L/h = 5$ E ratio = 4 for all theories.

CONCLUSIONS

In this study, the numerical and analytical analyses for free vibration of FGB based on CBT, FSDT, and HSDT were established. The motion equations were found by using Hamilton's principle. Numerical and analytical results express that the power index value, deformation theories, aspect ratio, and modulus ratio have a significant effect on free vibration and can be summarized as the following:

In calculation of dimensionless natural frequency, when the aspect ratio (L/H) ≥ 20 , the difference between CBT and all types of Timoshenko's beam theories are reduced and this makes the effect of shear is neglected the way it is in Euler's model.

The dimensionless natural frequency was calculated numerically by the Ansys program and it is similar to that one which was calculated analytically by FSDT.

As the power index value increases, the dimensionless natural frequency decreases when modulus ratio > 1 and increases if modulus ratio < 1 .

When the aspect ratio increases, the dimensionless natural frequency will increase too.

When the power index value remains constant, the dimensionless natural frequency increases when the modulus ratio increases for all aspect ratios and all theories.

When the three theories (CBT, FSDT, and HSDT) are compared, it can be found that the neglecting of the shear's effect leads to an increase in the dimensionless frequency as it is in the CBT. Therefore, the above theories (TBT, FSDT, and Ansys) led to reducing the vibration problem.

AUTHORS' CONTRIBUTION

Conceptualization: Neamah RA, Nassar AA and Alansari LS; **Methodology:** Neamah RA, Nassar AA and Alansari LS; **Investigation:** Neamah RA; **Writing – Original Draft:** Neamah RA; **Writing – Review and Editing:** Neamah RA; **Funding Acquisition:** Neamah RA; **Resources:** Neamah RA; **Supervision:** Nassar AA and Alansari LS.

DATA AVAILABILITY STATEMENT

All dataset were generated/analyzed in the current study.

FUNDING

Not applicable.

ACKNOWLEDGEMENTS

Not applicable.

REFERENCES

- AlSaid-Alwan HHS, Avcar M (2020) Analytical solution of free vibration of FG beam utilizing different types of beam theories: A comparative study. *Comput Concr* 26(3):285-292. <https://doi.org/10.12989/cac.2020.26.3.285>
- Alshorbagy AE, Eltaher MA, Mahmoud FF (2011) Free vibration characteristics of a functionally graded beam by finite element method. *Applied Mathematical Modelling* 35(1):412-425. <https://doi.org/10.1016/j.apm.2010.07.006>
- Amara K, Bouazza M, Fouad B (2016) Postbuckling Analysis of Functionally Graded Beams Using Nonlinear Model. *Period Polytech Mech Eng* 60(2):121-128. <https://doi.org/10.3311/PPme.8854>
- Anandrao KS, Gupta RK, Ramachandran P, Rao GV (2012) Free vibration analysis of functionally graded beams. *Def Sci J* 62(3):139-146. <https://doi.org/10.14429/dsj.62.1326>
- Avcar M, Alwan HHA (2017) Free Vibration of Functionally Graded Rayleigh Beam. *Int J Eng Appl Sci* 9(2):127-137. <https://doi.org/10.24107/ijjeas.322884>
- Avcar M, Hadji L, Civalek Ö (2021) Natural frequency analysis of sigmoid functionally graded sandwich beams in the framework of high order shear deformation theory. *Compos Struct* 276:114564. <https://doi.org/10.1016/j.compstruct.2021.114564>
- Aydogdu M (2009) A general nonlocal beam theory: Its application to nanobeam bending, buckling and vibration. *Phys E: Low-Dimens Syst Nanostructures* 41(9):1651-1655. <https://doi.org/10.1016/j.physe.2009.05.014>
- Aydogdu M, Taskin V (2007) Free vibration analysis of functionally graded beams with simply supported edges. *Materials and Design* 28(5):1651-1656. <https://doi.org/10.1016/j.matdes.2006.02.007>
- Bouamama M, Refassi K, Elmeiche A, Megueni A (2018) Dynamic Behavior of Sandwich FGM Beams. *Mech Mech Eng* 22(4):919-930. <https://doi.org/10.2478/mme-2018-0072>
- Chauhan PK, Khan IA (2014) Review on Analysis of Functionally Graded Material Beam Type Structure. *Int J Adv Mech Eng* 4(3):299-306.
- Ebrahimi F, Barati MR (2018) A modified nonlocal couple stress-based beam model for vibration analysis of higher-order FG nanobeams. *Mech Adv Mater Struct* 15(13):1121-1132. <https://doi.org/10.1080/15376494.2017.1365979>

- El Bikri K, Zerkane A, Benamar R (2012) Large amplitude free vibration analysis of functionally graded beams using an homogenisation procedure. published by EDP Sci 1:1003. <https://doi.org/10.1051/mateconf/20120110003>
- El-Galy IM, Bassiouny BI, Ahmed MH (2018) Empirical model for dry sliding wear behaviour of centrifugally cast functionally graded Al/SiCp composite. *Key Eng Mater* 786:276-285. <https://doi.org/10.4028/www.scientific.net/KEM.786.276>
- Elmeiche A, Megueni A, Lousdad A (2016) Free Vibration Analysis of Functionally Graded Nanobeams Based on Different Order Beam Theories Using Ritz Method. *Period Polytech Mech Eng* 60(4):209-219. <https://doi.org/10.3311/PPme.8707>
- Eltaher MA, Emam SA, Mahmoud IF (2012) Free vibration analysis of functionally graded size-dependent nanobeams. *Appl Math Comput* 218(14):7406-7420. <https://doi.org/10.1016/j.amc.2011.12.090>
- Faeouq W, Khazal H, Hassan AK (2019) Fracture analysis of functionally graded material using digital image correlation technique and extended element-free Galerkin method. *Opt Lasers Eng* 121:307-322. <https://doi.org/10.1016/j.optlaseng.2019.04.021>
- Fathi R, Ma A, Saleh B, Xu Q, Jiang J (2020) Investigation on mechanical properties and wear performance of functionally graded AZ91-SiCp composites via centrifugal casting. *Mater Today Commun* 24:101169. <https://doi.org/10.1016/j.mtcomm.2020.101169>
- Fouda N, El-midany T, Sadoun AM (2017) Bending, Buckling and Vibration of a Functionally Graded Porous Beam Using Finite Elements. *J Appl Comput Mech* 3(4):274-282. <https://doi.org/10.22055/jacm.2017.21924.1121>
- Ghadiri M, Jafari A (2018) A Nonlocal First Order Shear Deformation Theory for Vibration Analysis of Size Dependent Functionally Graded Nano beam with Attached Tip Mass: an Exact Solution. *J Solid Mech* 10(1):23-37. <https://doi.org/10.1001.1.20083505.2018.10.1.2.4>
- Hashemi SH, Khaniki HB, Khaniki HB (2016) Free Vibration Analysis of Functionally Graded Materials Non-uniform Beams. *Int J Eng Transactions: Aspects* 29(12):1734-1740. <https://doi.org/10.5829/idosi.ije.2016.29.12c.12>
- Kapuria S, Bhattacharyya M, Kumar AN (2008) Bending and free vibration response of layered functionally graded beams: A theoretical model and its experimental validation. *Compos Struct* 82(3):390-402. <https://doi.org/10.1016/j.compstruct.2007.01.019>
- Karamanli A (2016) Analysis of Bending Deflections of Functionally Graded Beams by Using Different Beam Theories and Symmetric Smoothed Particle Hydrodynamics. *Int J Eng Sci Technol* 2(3):105-117. <https://doi.org/10.19072/ijet.259394>
- Ke L-L, Yang J, Kitipornchai S (2010a) Nonlinear free vibration of functionally graded carbon nanotube-reinforced composite beams. *Compos Struct* 92(3):676-683. <https://doi.org/10.1016/j.compstruct.2009.09.024>
- Ke L-L, Yang J, Kitipornchai S (2010b) An analytical study on the nonlinear vibration of functionally graded beams. *Meccanica* 45(6):743-752. <https://doi.org/10.1007/s11012-009-9276-1>
- Khan AA, Alam MN, Rahman N, Wajid M (2016) Finite Element Modelling for Static and Free Vibration Response of Functionally Graded Beam. *Lat Am J Solids Struct* 13(4):690-714. <https://doi.org/10.1590/1679-78252159>
- Khazal H, Bayesteh H, Mohammadi S, Ghorashi SS, Ahmed A (2016) An extended element free Galerkin method for fracture analysis of functionally graded materials. *Mechanics of Advanced Materials and Structures* 23(5):513-528. <https://doi.org/10.1080/15376494.2014.984093>
- Khazal H, Hassan AKF, Farouq W, Bayesteh H (2019) Computation of Fracture Parameters in Stepwise Functionally Graded Materials Using Digital Image Correlation Technique. *Mech Adv Mater Struct* 8(1):344-354. <https://doi.org/10.1520/MPC20180175>

- Kirs M, Karjust K, Aziz I, Öunapuu E, Tungal E (2018) Free vibration analysis of a functionally graded material beam: evaluation of the Haar wavelet method. *Proc Estonian Acad Sci* 67(1):1-9. <https://doi.org/10.3176/proc.2017.4.01>
- Li W, Han B (2018) Research and Application of Functionally Gradient Materials. *IOP Conf Ser: Mater Sci Eng* 394:022065. <https://doi.org/10.1088/1757-899X/394/2/022065>
- Loy CT, Lam KY, Reddy JN (1999) Vibration of functionally graded cylindrical shells. *Int J Mech Sci* 41(3):309-324. [https://doi.org/10.1016/S0020-7403\(98\)00054-XMarzoq](https://doi.org/10.1016/S0020-7403(98)00054-XMarzoq)
- Z, Al-Ansari LS (2021) Calculating the fundamental frequency of power law functionally graded beam using Ansys software. *IOP Conf Ser: Mater Sci Eng* 1090:012014. <https://doi.org/10.1088/1757-899X/1090/1/012014>
- Mohammadimehr M, Mahmudian-Najafabadi M (2013) Bending and Free Vibration Analysis of Nonlocal Functionally Graded Nanocomposite Timoshenko Beam Model Rreinforced by SWBNNNT Based on Modified Coupled Stress Theory. *J Nanostruct* 3(4):483-492. <https://doi.org/10.7508/jns.2013.04.014>
- Nam VH, Vinh PV, Chinh NV, Thom DV, Hong TT (2019) A New Beam Model for Simulation of the Mechanical Behaviour of Variable Thickness Functionally Graded Material Beams Based on Modified First Order Shear Deformation Theory. *Materials* 12(3):404. <https://doi.org/10.3390/ma12030404>
- Neamah RA, Nassar AA, Alansari LS (2021) Buckling Simulation of Simply Support FG Beam Based on Different beam Theories. *Basrah Journal for Engineering Sciences* 21(3):10-24. <https://doi.org/10.33971/bjes.21.3.2>
- Neamah RA, Nassar AA, Alansari LS (2022) Review on Buckling and Bending Analysis of Functionally Graded Beam with and without Crack. *Basrah Journal for Engineering Sciences* 22(1): 69-77. <http://dx.doi.org/10.33971/bjes.22.1.8>
- Nguyen T-K, Nguyen TT-P, Vo T-P, Thai H-T (2015) Vibration and buckling analysis of functionally graded sandwich beams by a new higher-order shear deformation theory. *Compos B Eng* 76:273-285. <https://doi.org/10.1016/j.compositesb.2015.02.032>
- Paul A, Das D (2016) Free vibration analysis of pre-stressed FGM Timoshenko beams under large transverse deflection by a variational method. *Eng Sci Technol Int J* 19(2):1003-1017. <https://doi.org/10.1016/j.jestch.2015.12.012>
- Pradhan KK, Chakraverty S (2013) Free vibration of Euler and Timoshenko functionally graded beams by Rayleigh–Ritz method, *Compos B Eng* 51:175-184. <https://doi.org/10.1016/j.compositesb.2013.02.027Pradhan>
- N, Sarangi SK (2018) Free vibration Analysis of Functionally Graded Beams by Finite Element Method. *IOP Conf Ser: Mater Sci* 377:012211. <https://doi.org/10.1088/1757-899X/377/1/012211Rahimi>
- GH, Gazor MS, Hemmatnezhad M, Toorani H (2013) On the postbuckling and free vibrations of FG Timoshenko beams. *Compos Struct* 95:247-253. <https://doi.org/10.1016/j.compstruct.2012.07.034>
- Rahmani F, Kamgar R, Rahgozar R (2020) Finite Element Analysis of Functionally Graded Beams using Different Beam Theories. *Civ Eng J* 6(11):2086-2102. <https://doi.org/10.28991/cej-2020-03091604Rahmani>
- O, Pedram O (2014) Analysis and modeling the size effect on vibration of functionally graded nanobeams based on nonlocal Timoshenko beam theory. *Int J Eng Sci* 77:55-70. <https://doi.org/10.1016/j.ijengsci.2013.12.003>
- Saleh B, Jiang J, Fathi R, Xu Q, Wang L, Ma A (2020) Study of the microstructure and mechanical characteristics of AZ91–SiC_p composites fabricated by stir casting. *Archiv Civ Mech Eng* 20(3):71. <https://doi.org/10.1007/s43452-020-00071-9>
- Saleh B, Jiang J, Ma A, Song D, Yang D (2019) Effect of Main Parameters on the Mechanical and Wear Behaviour of Functionally Graded Materials by Centrifugal Casting: A Review. *Met Mater Int* 25(6):1395-1409. <https://doi.org/10.1007/s12540-019-00273-8>

- Saljooghi R, Ahmadian MT, Farrahi GH (2014) vibration and buckling analysis of functionally graded beams using reproducing kernel particle method. *Sci Iran* 21(6B):1896-1906.
- Sayyad AS, Ghugal YM (2018) Analytical solutions for bending, buckling, and vibration analyses of exponential functionally graded higher order beams. *Asian J Civ Eng* 19(5):607-623. <https://doi.org/10.1007/S42107-018-0046-Z>
- Senthamarakannan C, Ramesh R (2019) Evaluation of mechanical and vibration behavior of hybrid epoxy carbon composite beam carrying micron-sized CTBN rubber and nanosilica particles. *Proc Inst Mech Eng L: J Mater: Des Appl* 233(9):1738-1752. <https://doi.org/10.1177/1464420718784315>
- Şimşek M, Kocaturk T (2009) Free and forced vibration of a functionally graded beam subjected to a concentrated moving harmonic load. *Compos Struct* 90(4):465-473. <https://doi.org/10.1016/j.compstruct.2009.04.024>
- Şimşek M, Yurtcu HH (2013) Analytical solutions for bending and buckling of functionally graded nanobeams based on the nonlocal Timoshenko beam theory. *Composite Structures* 97:378-386. <https://doi.org/10.1016/j.compstruct.2012.10.038>
- Sola A, Bellucci D, Cannillo V (2016) Functionally graded materials for orthopedic applications – an update on design and manufacturing. *Biotechnol Adv* 34(5):504-531. <https://doi.org/10.1016/j.biotechadv.2015.12.013>
- Tarlochan F (2012) Functionally graded material: a new breed of engineered material. *J Appl Mech Eng* 1(5):1-2. <https://doi.org/10.4172/2168-9873.1000e115>
- Thai H-T, Vo TP (2012) Bending and free vibration of functionally graded beams using various higher-order shear deformation beam theories. *Int J Mech Sci* 62(1):57-66. <https://doi.org/10.1016/j.ijmecsci.2012.05.014>
- Vo T-P, Thai H-T, Nguyen T-K, Inam F (2013) Static and vibration analysis of functionally graded beams using refined shear deformation theory. *Meccanica* 49(1):155-168. <https://doi.org/10.1007/s11012-013-9780-1>
- Wattanasakulpong N, Prusty BG, Kelly DW, Hoffman M (2012) Free vibration analysis of layered functionally graded beams with experimental validation. *Materials and Design* 36:182-190. <https://doi.org/10.1016/j.matdes.2011.10.049>
- Wattanasakulpong N, Ungbhakorn V (2012) Free Vibration Analysis of Functionally Graded Beams with General Elastically End Constraints by DTM. *World J Mech*, 2(6):297-310. <https://doi.org/10.4236/wjm.2012.26036>
- Xu Q, Ma A, Li Y, Saleh B, Yuan Y, Jiang J, Ni C (2019) Enhancement of Mechanical Properties and Rolling Formability in AZ91 Alloy by RD-ECAP Processing. *Materials* 12(21):3503. <https://doi.org/10.3390/ma12213503>
- Zainy HZ, Alansari LS, Al-Hajjar AM, Mahdi M, Shareef S (2018) Analytical and numerical approaches for calculating the static deflection of functionally graded beam under mechanical load. *Int J Eng Technol* 7(4):3889-3896. <https://doi.org/10.14419/ijet.v7i4.20515>
- Zhao J, Wang Q, Deng X, Choe K, Xie F, Shuai C (2018) A modified series solution for free vibration analyses of moderately thick functionally graded porous (FGP) deep curved and straight beams. *Compos B Eng* 165:155-166 <https://doi.org/10.1016/j.compositesb.2018.11.080>